Check for updates

ASCE

A Social Welfare–Based Infrastructure Resilience Assessment Framework: Toward Equitable Resilience for Infrastructure Development

Sunil Dhakal, S.M.ASCE[1]; and Lu Zhang, A.M.ASCE[2]

Downloaded from ascelibrary.org by Florida International University on 12/05/22. Copyright ASCE. For personal use only; all rights reserved.

Abstract: Resilient infrastructure, which better withstands, adapts, and recovers from disasters, can limit disaster impacts, such as disruptions to infrastructure services and time and efforts needed for recovery. However, in the context of a disaster, the impacts on infrastructure are not evenly distributed across different communities. Thus, we need to account for such disparities (or inequalities) when assessing infrastructure resilience. To address this need, this paper proposes a social-welfare–based infrastructure resilience assessment (SW-Infra-RA) model for quantifying the collective resilience of infrastructure serving multiple communities. This model accounts for (1) disaster inequality—the unequal distributions of disaster impacts on infrastructure across different communities; and (2) disaster vulnerability—the disaster impacts on the infrastructure of communities that suffer from the most severe impacts—both of which have impacts on the collective resilience of infrastructure. A set of hypothetical and real case studies were conducted to illustrate the use of the proposed model in quantitatively assessing infrastructure resilience. This study contributes to the body of knowledge by providing a new infrastructure resilience assessment model that accounts for disaster inequality and vulnerability. The proposed model has the potential to support the development and investment of infrastructure in a more equitable manner; it facilitates equitable resilience in future infrastructure planning and development.
DOI: 10.1061/(ASCE)NH.1527-6996.0000597. *© 2022 American Society of Civil Engineers.*

Author keywords: Infrastructure resilience assessment; Equitable resilience; Equity; Vulnerability; Disaster inequality; Social welfare functions.

Introduction

From meeting everyone's basic needs to supporting trade, economy, and technology advancement, infrastructure services are the key enablers of human well-being and development. With climate change and the growth in intensities and frequencies of natural hazards, there are increasing urgency and priority on investing in and developing resilient infrastructure (Hallegatte et al. 2019). A resilient infrastructure with high-quality and robust structural components can potentially limit the impacts of natural hazards in terms of physical damage, economic losses, and functional disruptions (Braese et al. 2019). Over the last two decades, significant efforts have been made for the investment, development, and maintenance of resilient infrastructure to better withstand, adapt to, and rapidly recover from disaster impacts. However, in the context of a disaster, large disparities may exist in the levels of damage and/or recovery processes of the infrastructure across various communities. Such disparities may be caused by the differences in the severity of disaster exposure, and they may also be caused by the variations in the quality and adequacy of infrastructure services across different communities (Coleman et al. 2020). Some communities (e.g., wealthier communities) may have more investment in the development and rehabilitation of existing infrastructure (Hirsch et al. 2017; Nexus 2017). In contrast, some disaster-vulnerable communities, referring to those communities that suffer from the most severe disaster impacts, may struggle with unmet infrastructure needs, such as unreliable electric power systems, lack of adequate water and sanitation systems, overstrained transportation networks, and degraded school buildings, even before the disaster (Huang and Taylor 2019; Hallegatte et al. 2019). Underinvestment, insufficient maintenance, and mismanagement are some of the key factors that result in inadequate infrastructure services in these vulnerable communities (Hallegatte et al. 2019). In addition, research (e.g., SMASHA 2017; Ward and Shively 2016; Yoon 2012; Flanagan et al. 2011) shows that such disaster vulnerability is associated with social vulnerability. Socially vulnerable communities may include those with higher percentages of economically disadvantaged, racial and ethnic minorities, elderly, uninsured, homeless, disabled, those with chronic health conditions, and those with language barriers (Rao et al. 2019; AJMC 2006). These communities often have the fewest resources for disaster preparedness, are located in disaster-prone areas, and lack the social, political, and economic capital needed to withstand, adapt to, and recover from a disaster. As a result, they are more likely to suffer from severe disaster impacts (e.g., higher percentages of power outages or traffic disruptions, longer recovery time) (Hallegatte et al. 2019; SAMSHA 2017). Due to the unequal distributions of disaster impacts and more severe impacts on the infrastructure of disaster-vulnerable communities, there is sorely a need to systematically integrate disaster inequality and vulnerability with infrastructure resilience assessment.

Despite such a need, we have identified a number of knowledge gaps in the domain of infrastructure resilience assessment. Over the last two decades, many research studies (e.g., Panteli et al. 2017;

[1]Ph.D. Candidate, Dept. of Civil and Environmental Engineering, Florida International Univ., 10555 West Flagler St., EC 2900, Miami, FL 33174.

[2]Assistant Professor, Moss Dept. of Construction Management, Florida International Univ., 10555 West Flagler St., EC 2935, Miami, FL 33174 (corresponding author). ORCID: https://orcid.org/0000-0001-9890-1365. Email: luzhang@fiu.edu

Note. This manuscript was submitted on October 22, 2021; approved on August 4, 2022; published online on November 17, 2022. Discussion period open until April 17, 2023; separate discussions must be submitted for individual papers. This paper is part of the ***Natural Hazards Review***, © ASCE, ISSN 1527-6988.

Tonn et al. 2020; Cimellaro et al. 2010; Mao and Li 2018; Yang et al. 2018) have focused on developing models or frameworks to measure or assess infrastructure resilience. Various approaches or methods have been used in resilience assessment, such as simulation-based approaches (e.g., Hossain et al. 2019), mathematical approaches (e.g., Cimellaro et al. 2010), index-based approaches (e.g., Fisher and Norman 2010), and data-driven approaches (e.g., Zhu et al. 2017). These studies have provided valuable contributions toward advancing the understanding and facilitating infrastructure resilience. However, there remains limited research that integrates the disparity and vulnerability in disaster impacts with infrastructure resilience assessment. In other words, there is a lack of studies that (1) measure the unequal distributions of disaster impacts (e.g., infrastructure functional loss, infrastructure recovery time) across different communities and potentially more severe impacts on vulnerable communities; and (2) investigate how they would impact the collective resilience of infrastructure that serves multiple communities.

To address these knowledge gaps, we propose a social-welfare–based infrastructure resilience assessment (SW-Infra-RA) model that assesses the collective resilience of infrastructure serving multiple communities by accounting for (1) disaster inequality—the unequal distributions of disaster impacts on infrastructure across various communities; and (2) disaster vulnerability—the disaster impacts on the infrastructure of the communities that suffer from the most severe impacts. The proposed model is theoretically grounded on the social welfare theory and social welfare functions. It also adapts the methods from Bruneau et al.'s (2003) resilience triangle framework and Cutter et al.'s (2003) Social Vulnerability Index. The proposed model aims to address the following research questions: How to quantitatively measure the unequal distributions of disaster impacts on infrastructure across different communities?; How to quantitatively measure the potentially more severe disaster impacts on the infrastructure of vulnerable communities?; and How to mathematically integrate the disparity and vulnerability in disaster impacts with infrastructure resilience assessment? This paper focuses on presenting and discussing the conceptual notions and mathematical functions in the SW-Infra-RA model. The remainder of the paper first reviews and discusses the relevant literature. It then presents the SW-Infra-RA model, including all the mathematical functions in the model. At the end, it discusses two sets of case studies (including a hypothetical and a real case study) to illustrate the use of the SW-Infra-RA model in determining the collective resilience of infrastructure serving multiple communities.

Literature Review

Infrastructure Resilience Assessment in Disaster Literature

Over the last two decades, the concept of infrastructure resilience has gained significant attention from scientific scholars and researchers around the world (Karamouz et al. 2019; Cimellaro et al. 2010). The concept of "resilience" was first introduced by Holling (1973) to describe the "persistence of relationships within a system" and the ability of the system to "absorb changes of state variables, driving variables, and parameters, and still persist" (Holling 1973). Holling (1996) also explained the difference between engineering resilience and ecological resilience. Ecological resilience measures how a system can persist by absorbing changes and disturbances, while engineering resilience measures the capacity of the system to recovery to its original functional level after a disturbance. Integrating these definitions, infrastructure resilience is typically defined as the ability of infrastructure to anticipate and absorb the shock, adapt to, and quickly recover to its original functional level (Berkeley et al. 2010).

Over the years, many resilience assessment frameworks have been proposed to assess the resilience of different types of infrastructure, such as transportation infrastructure (e.g., Tonn et al. 2020), electric power infrastructure (e.g., Hossain et al. 2019), water and sanitation infrastructure (e.g., Assad et al. 2019), and telecommunication infrastructure (e.g., Mawgoud et al. 2021). These studies used different approaches to assess infrastructure resilience, including simulation-based approaches (e.g., Hossain et al. 2019; Hosseini and Barker 2016; Lam and Tai 2018), mathematical approaches (e.g., Cimellaro et al. 2010; Shin et al. 2018; Bruneau et al. 2003), index-based approaches (e.g., Rehak et al. 2019; Petit et al. 2012; Fisher and Norman 2010), and data-driven approaches (e.g., MacKenzie and Barker 2013; Zhu et al. 2017).

Simulation-based approaches were mostly employed in the resilience assessment of system networks, such as water supply networks (e.g., Assad et al. 2019), electric grid networks (e.g., Hossain et al. 2019), and transportation networks (e.g., Hosseini and Barker 2016). In these studies, Bayesian networks, Monte Carlo simulation, and Fuzzy models were commonly used for the analysis. For example, Hossain et al. (2019) employed Bayesian networks to quantitatively assess the resilience of electric infrastructure systems. Similarly, Hosseini and Barker (2016) built a resilience assessment framework to quantify the resilience capacity of an inland waterway network using Bayesian networks. Nogal et al. (2017) proposed a resilience assessment framework to estimate the resilience of a transportation network impacted by extreme events using the Monte Carlo simulation method. Lam and Tai (2018) used a Fuzzy modeling approach to model the interdependencies between entities in infrastructure networks by simulating the effects of disruptions.

Using mathematical approaches, the resilience of infrastructure can be assessed through mathematical structures, notions, or equations. The mathematical approaches can be classified into deterministic (e.g., Bruneau et al. 2003; Cimellaro et al. 2010) and probabilistic (e.g., Decò et al. 2013; Nogal et al. 2017) approaches. The deterministic approach utilizes the value of the input parameters to obtain a precise outcome without accounting for uncertainties. In contrast, the probabilistic approach can model the uncertainties that exist in the inputs of metrics to obtain the distributions of infrastructure failure and recovery (Mottahedi et al. 2021). For example, Cimellaro et al. (2010) proposed a comprehensive conceptual model that includes a loss estimation model and a recovery model to quantitatively assess the seismic resilience of a network of health care facilities. Decò et al. (2013) used a probabilistic approach to assess the seismic resilience of bridges.

Using index-based approaches, a resilience index is developed by identifying and aggregating a set of indicators that represent the characteristics of infrastructure resilience. The resilience index can then be used to compare or rank the resilience of several infrastructure alternatives by collecting the data of each infrastructure alternative. To frame the resilience index, both qualitative (measured with ordinal or nominal scales) and quantitative indicators (measured with interval or ratio scales) can be used (Cardoni et al. 2020). Multiple resilience indexes have been developed over the years, such as the Resilience Star developed by the Department of Homeland Security (Kangior 2013), the US Resiliency Council (USRC) Building Rating System (USRC 2021), the Resilience-based Earthquake Design Initiative (REDi) rating system (ARUP 2021), and the Resilience Action List (RELi) rating system (GBCI 2021). Similarly, many researchers have used index-based approaches to develop different infrastructure resilience assessment

Downloaded from ascelibrary.org by Florida International University on 12/05/22. Copyright ASCE. For personal use only; all rights reserved.

frameworks. For example, Yang et al. (2018) developed the Resilience Index Considering Duration of events (RICD), which assesses the resilience of power transmission systems under the typhoon weather. Argyroudis et al. (2021b) built a cost-based resilience index that quantifies the seismic resilience of bridges. Cardoni et al. (2020) developed the Power Resilience Index (PRI) that assesses the seismic resilience of urban electric power distribution systems.

Data-driven approaches refer to those methods that rely on collecting, analyzing, and interpreting data to derive insight, knowledge, or solutions. This approach can be used to develop new models to calibrate and reduce uncertainties when assessing infrastructure resilience (Argyroudis et al. 2021a). By deriving knowledge from a large amount of data, the data-driven approach may provide a high level of reliability that cannot be achieved through other conventional scientific approaches (Maass et al. 2018). In the last decade, with the advancement of data analytics techniques, there has been a growing tendency of adopting data-driven approaches for resilience assessment. For example, Argyroudis et al. (2021a) proposed a data-driven resilience assessment framework for critical transportation infrastructure that is exposed to multiple hazards by interactively analyzing multiscale monitoring data (e.g., terrestrial data, airborne data), crowd data, and environmental measurements. Chandramouleeswaran and Tran (2018) used a data-driven approach for quantitatively assessing the resilience of air transportation networks using publicly available data (e.g., total cancellation flights, average flight delay).

The existing research has offered valuable contributions to advance the understanding and methods of assessing infrastructure resilience. However, one of the major concerns that lie behind the demand for better resilience assessment is the need to pay more attention to equity and vulnerability in resilience assessment (Meerow et al. 2019; Meerow and Newell 2019). Much of the resilience assessment literature focuses on evaluating the performance of a whole (e.g., a complete infrastructure network) while lacking consideration of the inequalities and trade-offs among different parts that compose the whole. Some resilience assessment studies (e.g., RF 2021; GBCI 2021) proposed to integrate equity as one dimension or a characteristic of resilience. These studies tend to mix the conceptualizations of equity and resilience and simplify their relationships. Although disaster resilience and equity are interconnected, they are not the same. Integrating equity with resilience requires us to explicitly assess the unequal distributions of disaster impacts on various communities and evaluate the different levels of vulnerability that these communities face (Wescoat et al. 2018). There is, thus, a need to develop a new resilience assessment framework that assesses the collective infrastructure resilience while accounting for the disparities among the communities and potentially severe impacts on the infrastructure of vulnerable communities.

Resilience Triangle Framework

The resilience triangle framework was based on the work by Bruneau et al. (2003), who defined and quantitatively measured the seismic resilience of communities. According to Bruneau et al. (2003), a resilient system has three key characteristics: (1) reduced failure probabilities, (2) reduced consequences from the failures, and (3) reduced time to recovery. They then proposed to measure the resilience of a community by defining and measuring the area of a resilience triangle (Fig. 1). In the resilience triangle, the vertical axis represents the quality of infrastructure in a community [Q(t)], which varies with time. Q(t) ranges from 0% to 100%, where 100% represents no degradation in infrastructure quality or service, and

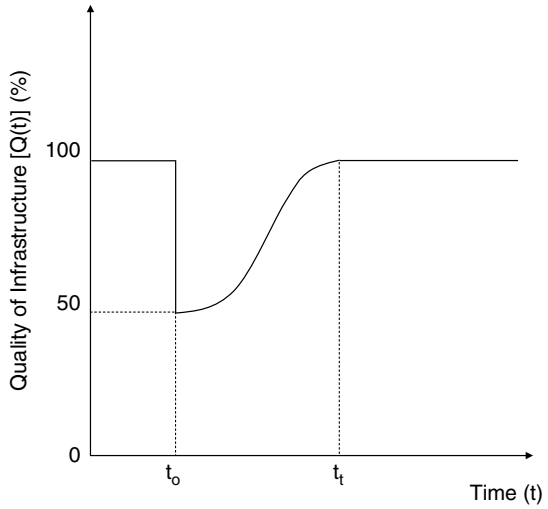

Fig. 1. A conceptual diagram of a resilience triangle. [M. Bruneau, S. E. Chang, R. T. Eguchi, G. C. Lee, T. D. O'Rourke, A. M. Reinhorn, M. Shinozuka, K. Tierney, W. A. Wallace, and D. Von Winterfeldt, "A framework to quantitatively assess and enhance the seismic resilience of communities." *Earthquake spectra* 19 (4): 125–131, © 2003 by SAGE, reprinted by permission of SAGE Publications, Ltd.]

0% means no infrastructure service is available. An earthquake occurring at time t_o would cause damage to infrastructure so that the quality of infrastructure service is immediately reduced. Restoration of infrastructure is a process that takes time, and the quality of infrastructure gradually increases as the restoration process goes on. The infrastructure is completely recovered to its original functional level at time t_t. Therefore, the community loss of resilience is determined by aggregating the degradation of the quality of infrastructure over the total recovery time ($t_t - t_o$).

Over the last two decades, many research studies have been conducted to apply or adapt Bruneau et al.'s (2003) framework in assessing the resilience of various types of infrastructure, such as healthcare facilities (Shang et al. 2020), electric power systems (Ouyang and Duenas-Osorio 2014), and transportation infrastructure (Argyroudis et al. 2021b). The framework has also been adapted to analyze disruptions caused by disasters other than earthquakes, such as hurricanes (e.g., Ouyang and Duenas-Osorio 2014) and flooding (e.g., Zamanian et al. 2020).

Social Welfare Functions

Welfare economics is the study of how the distribution of resources and goods impacts social welfare; it evaluates well-being (welfare) at the aggregate level (Deardorff 2016). In welfare economics, several functions were proposed to evaluate or compare alternative social states (e.g., income distributions, life expectancy, literacy rate), and these functions are called social welfare functions (SWFs) (Weymark 2016). An SWF can be thus defined as a function that measures or ranks the collective welfare of the society in different social states (Arrow 1963). It can be used to determine the optimal distribution of well-being among individuals to achieve the maximum well-being for the whole society (Arrow 1963). In an SWF, well-being is generally expressed in terms of utilities (e.g., incomes, benefits) or preferences.

In welfare economics literature, SWFs can be generally classified into (1) the Bergson–Samuelson SWFs, (2) the Arrow SWFs, and (3) Cardinal SWFs. The Bergson–Samuelson SWFs determine the social preference (in the form of social ordering or ranking) of

Downloaded from ascelibrary.org by Florida International University on 12/05/22. Copyright ASCE. For personal use only; all rights reserved.

alternative social states (Weymark 2016) based on individual utilities (e.g., income, life expectancy). Through the functions, the individual utilities in alternative social states are first determined and further aggregated to determine the collective social preference. With the Arrow SWFs, the social preference of alternative social states is determined as a function of individual preferences (Weymark 2016). Unlike the Bergson–Samuelson SWFs, the Arrow SWFs only use information about individual preferences to determine social preferences.

Cardinal SWFs, on the other hand, are functions that determine the collective welfare (in the form of numerical value) based on individual utilities. They do not necessarily require comparisons among individual utilities in alternative social states, and they yield a numerical representation of the collective welfare for each social state. Some of the Cardinal SWFs found in the literature include Utilitarian SWF (Harsanyi 1955), Rawlsian SWF (Rawls 1971), Bernoulli–Nash SWF (Jagtenberg 2017), Sen's SWF (Sen 1997), and Atkinson and Brandolini SWF (Atkinson and Brandolini 2010). The Utilitarian SWF measures social welfare as the average welfare of the individuals in the society. With the Utilitarian SWF, the collective social welfare of a society increases if the welfare of any individual increases and none decreases, with everyone indifferent (Harsanyi 1955; Schneider and Kim 2020). This function does not account for the equality of welfare (e.g., fair distributions of income) among the individuals in a society. With the Rawlsian SWF, the welfare of the society is determined by the welfare of the individuals with the lowest welfare in a society (Rawls 1971). According to the Rawlsian SWF, social welfare increases if the welfare of the poorest individuals increases; it does not consider the welfare of other individuals in the society. Similar to Utilitarian SWF, the Rawlsian SWF does not consider equality in welfare distributions in a society. The Bernoulli–Nash SWF, in general, can be seen as the mixture of the Rawlsian and the Utilitarian SWFs. With the Bernoulli–Nash SWF, the collective social welfare is calculated as the product of all individual welfare (Jagtenberg 2017).

To account for inequality in welfare distributions, Sen (1997) proposed an SWF (Sens's SWF) that accounts for unequal distributions of welfare across the individuals in a society. In Sen's SWF, a Gini coefficient is used to measure welfare inequality. Sen's SWF determines social welfare as the product of the average welfare of all individuals and an inequality indicator. According to Sen's SWF, social welfare increases if the fairness in distributing the welfare increases. However, with Sen's SWF, it is possible that the total amount of welfare increases at the expense of increased equality and reduced average welfare. In other words, social welfare could increase by allowing all individuals to be equally poorer (Mostafa and El-Gohary 2014). Thus, to account for poverty in social welfare, a poverty line is defined based on the minimum amount of income an individual or a household needs to meet their basic needs (Callan and Nolan 1991). The individual or household whose income falls below the poverty line is considered as being poor. Leveraging the poverty line, Atkinson and Brandolini (2010) proposed an SWF that accounts for the poorest individuals with the minimum welfare in a society.

Over the year, scholars in the domains of social science and economics have used the SWFs to solve various problems, such as reducing health inequalities (Dolan and Robinson 2001), assessing climate policies (Füssel 2006), and improving cost-benefit analysis (Adler 2017). In recent years, the SWFs have been further adapted to address issues in other domains, such as transportation, architecture, engineering, and construction. For example, Zhang and Sanake (2020) proposed a social welfare–based group comfort analysis model to measure the collective comfort level of a group of individuals in indoor environments. Kinjo and Ebina (2017) developed a mathematical model based on Utilitarian SWF and Nash SWF to determine autonomous vehicle (AV) driving behaviors by evaluating individual utilities of passengers inside the AV and pedestrians on a street. Mostafa and El-Gohary (2014) presented a social welfare–based sustainability benefit analysis model that evaluates the distribution of benefits of infrastructure project alternatives to their stakeholders by accounting for both equality and poverty in benefit distributions.

Social Inequality Measurements

Inequality refers to an absence of equal distributions of goods, services, opportunities, rights, and/or dignity (UNCTAD 2021). Inequality is often measured by assigning a certain value to a specific distribution in order to facilitate direct and objective comparisons across different distributions (UNCTAD 2021). There are multiple methods to measure inequality, and these methods can be categorized as using "ratios" or using "indices."

Measuring inequality through "ratios" is a relatively easy and straightforward method. The most commonly used ratios for measuring inequality are the 20/20 ratio and the Palma ratio. The 20/20 ratio represents the ratio of the average income of the richest 20% of the population to the average income of the poorest 20% of the population (Afonso et al. 2015; UNCTAD 2021). Palma ratio is defined as the ratio of the total income of the richest 10% of households to the poorest 40% of households (Afonso et al. 2015; UNCTAD 2021). Although ratios are relatively easy to understand, these methods do not measure how social welfare (e.g., income) is equally or unequally distributed across the population. For example, they do not consider the welfare (e.g., income) distributions within the highest and lowest percentiles of the population (Trapeznikova 2019).

As compared to "ratios," "indices" are more commonly used to measure inequality. Some of the popular indices are Atkinson's index (Afonso et al. 2015), Hoover index (Hoover 1941), Theil index (Theil 1967), and Gini index (Trapeznikova 2019). Atkinson's index is a welfare–based measure of inequality, and it represents the percentage of total income that could be sacrificed to have more equal shares of income among individuals without reducing social welfare (Afonso et al. 2015). The Hoover index, also known as the Schutz index, defines inequality as the share of total income that needs to be redistributed from the population with income above mean to those with income below the mean to achieve income equality (Afonso et al. 2015). A higher value of the Hoover index indicates a higher level of inequality, and more redistributions are needed to achieve equality. The Theil index belongs to general entropy (GE) measures; it measures an entropic "distance" the population is away from the ideal equitable state, in which all individuals have the same income (Conceição and Ferreira 2000). Since the Theil index is not a relative measure of inequality, the values of this index are not always comparable across different groups and sizes of populations (Trapeznikova 2019). The Gini index is the most widely used and recognized measure of inequality (Trapeznikova 2019). It can be used to measure the inequality of any distribution. One of the benefits of using the Gini coefficient is to allow for direct comparisons of inequality states across different groups of populations, irrespective of their sizes (Afonso et al. 2015). A higher Gini coefficient value indicates higher inequality. The Gini coefficient has been used in measuring inequality in various domains, such as energy consumption (Jacobson et al. 2005), water consumption (Wang et al. 2012), indoor environmental quality (Zhang and Sanake 2020), and healthcare resource allocation (Jian et al. 2015).

Downloaded from ascelibrary.org by Florida International University on 12/05/22. Copyright ASCE. For personal use only; all rights reserved.

In our study, we chose to adapt the Gini coefficient in measuring the inequality of disaster impacts for the following reasons: (1) it allows for the measurement of distributions of disaster impacts across multiple communities, (2) it allows for comparisons of distributions of disaster impacts across communities with different sizes of population, (3) it is not affected by the characteristics (e.g., poverty) of the communities, and (4) it is relatively straightforward and easy to interpret.

Proposed Infrastructure Resilience Evaluation Framework

The proposed SW-Infra-RA model aims to define the collective resilience of infrastructure that serves multiple communities by integrating (1) disaster inequality—the unequal distributions of disaster impacts on infrastructure across the various communities; and (2) disaster vulnerability—the disaster impacts on the infrastructure of the communities that suffer from the most severe impacts. The framework is grounded in the social welfare theory and functions. It also adapts the methods from Bruneau et al.'s (2003) resilience triangle framework and Cutter et al.'s (2003) Social Vulnerability Index. The model assesses the collective resilience of infrastructure in five main steps, including (1) determining disaster impacts on individual communities, (2) modeling inequality of disaster impacts, (3) modeling vulnerability in disaster impacts, (4) measuring collective disaster impacts, and (5) assessing collective infrastructure resilience. The following sections discuss each step in detail.

Determining Disaster Impacts on Individual Communities

Disasters may cause severe damage to infrastructure, resulting in the reduction of its functionality, and it may take weeks or months to restore the infrastructure to its original functional level. According to Bruneau et al.'s (2003) resilience triangle framework, such characterization of infrastructure performance during a disaster leads to a broader conceptualization of resilience. Resilience can be understood as the ability of infrastructure (1) to reduce the possibility or extent of disaster impacts; and (2) to recover rapidly after a disaster (Bruneau et al. 2003). Such conceptualization of resilience is widely adopted in different disaster studies (e.g., Cimellaro et al. 2010; Rehak et al. 2019; Yang et al. 2018). Benchmarking the resilience triangle framework, two main types of indicators were identified to determine the disaster impacts on individual communities. These indicators include those that represent (1) the functional loss of infrastructure (e.g., percentage of power outages, percentage of road closures); and (2) the recovery time of infrastructure (e.g., time required to resume electric power services, time required to reopen roads).

Depending on the time of analysis, the selected disaster, the level of analysis (e.g., state level, county level, city level, community level), and data availability, there are two main methods for collecting the data for these indicators (i.e., functional loss and recovery time of infrastructure). For analyzing infrastructure resilience in the context of historical disasters, we can extract the relevant data that are available in public or private sources; the data can be collected directly from (1) public sources, such as state, county, or local Department of Emergency Management, Department of Transportation, Office of Communications Commission, or Office of Insurance Regulations; or (2) private sources, such as electric power companies and telecommunication companies. The data then need to be tabulated by the level of analysis (e.g., state, county, city, and community levels). For analyzing infrastructure resilience in the context of ongoing disasters, we need to collect firsthand data on infrastructure damage and recovery works by following damage assessment procedures and using the relevant tools and methods. For example, according to Federal Emergency Management Agency (FEMA)'s Preliminary Damage Assessment Guide (FEMA 2021), damage information of infrastructure needs to be captured by visually and technically inspecting and confirming the conditions of damaged infrastructure and identifying and documenting relevant disaster impacts (FEMA 2021).

In general, damage assessment is conducted using either a rapid approach or a detailed approach (Kwasinski 2011; Massarra 2012). Rapid damage assessment usually takes place as soon as conditions allow inspectors to operate after the occurrence of a disaster. It aims to generally estimate the nature and magnitude of damage and quickly inspect and assess the damage conditions. Thus, rapid assessment typically relies on an exterior observation and investigation of the structures. The magnitude of damage recorded on damage assessment forms (e.g., FEMA 2021) is typically a general estimate of the percentage of damage without accurate measurements (Massarra 2012). In recent years, many technologies have been proposed to facilitate the efficiency of rapid damage assessment. For example, GIS-based hazard modeling platforms (e.g., HAZUS) can be used to estimate potential damage from disasters, such as hurricanes and floods (CCSF 2021). Remote sensing technologies, which detect and monitor the physical characteristics of an area by measuring its reflected and emitted radiation from a certain distance, can be used to quickly estimate locations, causes, and severity of disaster damage conditions (Hao et al. 2020). If more detailed information is required regarding the damage conditions, rapid assessment should be followed by detailed assessments. Detailed damage assessment usually takes place about two to four weeks after the occurrence of a disaster (Massarra 2012). Detailed damage assessment aims to collect more thorough and accurate information regarding the impacts of a disaster, including estimation of loss value, determination of recovery progresses, and identification of recovery needs (Planitz 1999). Detailed damage assessment is based on the inspection of both structural (e.g., girder, column) and nonstructural components (e.g., railing, coating) of infrastructure (Massarra 2012). In our research context, both rapid and detailed assessments can be used to collect the data for determining disaster impacts on individual communities. The selection of the methods depends on the level of detail that is needed for infrastructure resilience analysis.

Modeling Inequality in Disaster Impacts

In our research context, disaster inequality refers to the unequal distributions of disaster impacts (i.e., functional loss, recovery time) on infrastructure of various communities. The unequal distribution of disaster impacts is analogous to the welfare inequality in a society, which is commonly measured through the Gini coefficient (Atkinson and Brandolini 2010). Thus, we adapted the Gini coefficient into the domain of infrastructure resilience assessment to measure the unequal distributions of disaster impacts (i.e., functional loss and recovery time) on infrastructure that serves multiple communities.

A Gini coefficient ranges from 0 to 1. A Gini coefficient of 0 means complete equality in disaster impacts—the infrastructure of all communities of analysis has the same level of functional loss, and/or it takes the same length of time for recovery. A Gini coefficient of 1 means complete inequality in disaster impacts—the infrastructure of only one community has the highest level of functional loss and requires the longest time in recovery. Graphically, the Gini coefficient can be represented through the Lorenz curve

Downloaded from ascelibrary.org by Florida International University on 12/05/22. Copyright ASCE. For personal use only; all rights reserved.

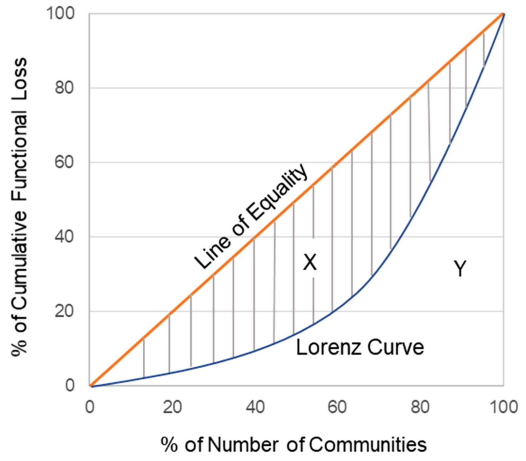

Fig. 2. A Lorenz curve for the distribution of infrastructure functional loss.

(Fig. 2). As per Fig. 2, it is measured by dividing the area between the Lorenz curve and the line of complete equality (i.e., Area X) by the area covered under the line of complete equality (i.e., Areas X + Y) (Wodon and Yitzhaki 2008; Mostafa and El-Gohary 2014). In the SW-Infra-RA model, the Lorenz curve illustrates the percentage of cumulative infrastructure functional loss (or recovery time) experienced by the percentage of communities in the analysis. For example, as per Fig. 2, a point on the Lorenz curve represents a statement such as, "the bottom 40% of all communities suffered from 10% of the total disaster impacts (e.g., functional loss, recovery time)." A Lorenz curve is always bowed downward from the line of equality or coincides with the line of equality if there exists complete equality among the individuals of analysis. The Lorenz curve being farther away from the line of equality indicates a higher level of inequality (i.e., the value of the Gini coefficient becomes closer to 1) and vice-versa. The Gini coefficient can also be defined through Eqs. (1) and (2), which are mathematically equivalent to the Lorenz curve. Eqs. (1) and (2) define the Gini coefficients that measure the unequal distributions of functional loss and recovery time (i.e., two main indicators of disaster impacts), respectively

$$G_{k(FL)} = \frac{\sum_{i=1}^{n}\sum_{j=1}^{n}|FL_{ik} - FL_{jk}|}{2n\sum_{i=1}^{n} FL_{ik}} \tag{1}$$

where $G_{k(FL)}$ = Gini coefficient for functional loss of a group k of multiple communities; FL_{ik} = functional loss of infrastructure in an individual community i of group k; FL_{jk} = functional loss of infrastructure in an individual community j of group k; and n = total number of communities in group k

$$G_{k(RT)} = \frac{\sum_{i=1}^{n}\sum_{j=1}^{n}|RT_{ik} - RT_{jk}|}{2n\sum_{i=1}^{n} RT_{ik}} \tag{2}$$

where $G_{k(RT)}$ = Gini coefficient for the recovery time of a group k of multiple communities; RT_{ik} = recovery time of infrastructure in an individual community i of group k; RT_{jk} = recovery time of infrastructure in an individual community j of group k; and n = total number of communities in group k.

Modeling Vulnerability to Disaster Impacts

In our research context, vulnerable communities in a disaster refer to those communities that suffer from the most severe impacts of a disaster. The concept of vulnerability to disaster impacts is analogous to the concept of poverty in welfare economics. Thus, benchmarking the methods for measuring poverty in welfare economics, we proposed a "line of vulnerability" to define and measure vulnerability in the SW-Infra-RA model. The line of vulnerability is a benchmark that indicates the vulnerability level of infrastructure serving different communities. If the value of disaster impacts (i.e., infrastructure functional loss and recovery time) is above the line of vulnerability, the community is identified as one of the vulnerable communities in the disaster. However, unlike the poverty line that has been extensively studied, there are no established methods to measure the line of vulnerability in the disaster domain. In our research, we adapted Cutter et al.'s (2003) work on social vulnerability. Cutter et al. (2003) constructed a social vulnerability index (SoVI) for all the counties in the United States based on county-level socioeconomic and demographic data. The counties with SoVI scores greater than the average plus standard deviation are identified as the most vulnerable counties. In our proposed model, the line of vulnerability can be defined as the sum of the mean and the standard deviation of infrastructure functional loss (or recovery time) experienced by the communities of analysis. Eqs. (3) and (4) define the line of vulnerability for functional loss and recovery time, respectively

$$LV_{(FL)_k} = \frac{1}{n}\sum_{i=1}^{n} FL_{ik} + \alpha S_{nk} \tag{3}$$

where $LV_{(FL)_k}$ = line of vulnerability for functional loss of infrastructure serving a group k of multiple communities; FL_{ij} = functional loss of infrastructure serving an individual community i of group k; n = total number of communities in group k; S_{nk} = standard deviation for the functional losses of infrastructure serving a group k of multiple communities; and α = a coefficient that controls the line of vulnerability ($0 \le \alpha \le 1$)

$$LV_{(RT)_k} = \frac{1}{n}\sum_{i=1}^{n} RT_{ik} + \beta S_{nk} \tag{4}$$

where $LV_{(RT)_k}$ = line of vulnerability for the recovery time of infrastructure serving a group k of multiple communities; RT_{ik} = recovery time of infrastructure serving an individual community i of group k; n = total number of communities in group k; S_{nk} = standard deviation for the recovery time of infrastructure serving a group k of multiple communities; and β = a coefficient that controls the line of vulnerability ($0 \le \beta \le 1$).

Depending on the context of analysis, users of the model have the flexibility to define and control the line of vulnerability through the coefficients of α and β. If the value of α (or β) is close to 0, the line of vulnerability is close to the average value. This means the criterion or benchmark for vulnerability is stringent, i.e., approximately half of the communities whose damage (or recovery time) is above the average will be accounted as vulnerable communities. If the value of α (or β) is close to 1, the line of vulnerability is close to the average value plus standard deviation. This means the criterion or benchmark for vulnerability is loose as a relatively smaller number of communities will be accounted as vulnerable communities. Defining such a line of vulnerability is important in identifying those communities that experience the most severe impacts during a disaster, and this could allow decision makers to prioritize efforts and investments in those communities in disaster assistance, recovery, and/or future mitigation efforts.

Downloaded from ascelibrary.org by Florida International University on 12/05/22. Copyright ASCE. For personal use only; all rights reserved.

Downloaded from ascelibrary.org by Florida International University on 12/05/22. Copyright ASCE. For personal use only; all rights reserved.

Measuring Collective Disaster Impacts

The SW-Infra-RA model measures the collective disaster impacts on infrastructure that serves multiple communities based on the distribution of impacts among individual communities. If we want to reduce the overall impact of a disaster, attention must be given to improving the overall equity and reducing the sensitivity of vulnerable communities to disasters (Nicholson 2014). Previous studies (e.g., Tselios and Tompkins 2019; Ward and Shively 2016) also show that higher inequality is associated with worse losses from disasters. Thus, when modeling the collective disaster impacts, we can assume that inequality and vulnerability are both unfavorable situations. Inequality and vulnerability will then be accounted for as factors that will further augment the collective disaster impacts.

In the SW-Infra-RA model, the function of collective disaster impacts includes the collective functional loss (CFL) function [Eq. (5)] and the collective recovery time (CRT) function [Eq. (6)]. Both functions incorporate the unequal distributions of disaster impacts on infrastructure serving multiple communities and the potentially severe impacts on infrastructure in vulnerable communities. These two functions are developed by adapting the SWFs (e.g., Mostafa and El-Gohary 2014; Zhang and Sanake 2020). The equation for the CFL function is presented as

$$CFL_k = \frac{1}{n}\sum_{i=1}^{n} FL_{ik} \times (1 + \gamma G_{k(FL)}) + \delta \frac{1}{n}\sum_{i=1}^{n} \max[0, (FL_{ik} - LV_{(FL)_k})] \quad (5)$$

where CFL_k = the CFL of the infrastructure that serves a group k of multiple communities; FL_{ik} = the functional loss of the infrastructure that serves an individual community i of group k; n = the total number of communities; $G_{k(FL)}$ = the Gini coefficient for the functional loss of group k; $LV_{(FL)_k}$ = the line of vulnerability for functional loss of infrastructure serving a group k of multiple communities; γ = a coefficient that controls the degree of accounting for inequality in augmenting the disaster impacts ($0 \le \gamma \le 1$); and δ = a coefficient that controls the degree of accounting for vulnerability in augmenting the disaster impacts ($0 \le \delta \le 1$).

Similarly, the equation for the CRT function is presented as

$$CRT_k = \frac{1}{n}\sum_{i=1}^{n} RT_{ik} \times (1 + \lambda G_{k(RT)}) + \mu \frac{1}{n}\sum_{i=1}^{n} \max[0, (RT_{ik} - LV_{(RT)_k})] \quad (6)$$

where CRT_k = the CRT of the infrastructure that serves a group k of multiple communities; RT_{ik} = the recovery time of the infrastructure that serves an individual community i of group k; n = the total number of communities; $G_{k(RT)}$ = the Gini coefficient for the recovery time of group k; $LV_{(RT)_k}$ = the line of vulnerability for the recovery time of infrastructure serving a group k of multiple communities; λ = a coefficient that controls the degree of accounting for inequality in augmenting the disaster impacts ($0 \le \lambda \le 1$); and μ = a coefficient that controls the degree of accounting for vulnerability in augmenting the disaster impacts ($0 \le \mu \le 1$).

Each of the CFL and the CRT functions consist of a subfunction for inequality and a subfunction for vulnerability. The inequality subfunction penalizes the unequal distributions of disaster impacts across different communities. In other words, inequality further augments the collective disaster impacts on these communities. The inequality is measured through the Gini coefficient [$G_{k(FL)}$, $G_{k(RT)}$] using Eq. (1) or Eq. (2). Additionally, a coefficient γ (or λ) is introduced to allow users to adjust the degree of penalizing unequal distributions of disaster impacts. The value of γ (or λ) ranges from 0 to 1, where γ (or λ) = 1 represents the full extent of penalization, and γ (or λ) = 0 represents no penalization at all. Thus, users of the model have the flexibility in determining to what extent they want to account for the inequality factor in infrastructure resilience assessment.

The vulnerability subfunction acknowledges that the potentially severe disaster impacts on the infrastructure of vulnerable communities could compromise the overall infrastructure resilience and should be penalized when assessing the collective resilience of infrastructure. In other words, more severe impacts on some vulnerable communities further augment the collective disaster impacts on all communities of analysis. In this function, a coefficient δ (or μ) is introduced, and it allows users to control the degree of accounting for vulnerability in collective disaster impacts. The value of δ (or μ) ranges from 0 to 1, where δ (or μ) = 1 represents the full extent of penalization, and δ (or μ) = 0 represents no penalization at all. Thus, users may have the flexibility in determining to what extent they want to account for the vulnerability factor in infrastructure resilience assessment.

Assessing Collective Infrastructure Resilience

The collective infrastructure resilience assessment function aims to measure the collective infrastructure resilience based on the collective disaster impacts—CFL and CRT. The function was developed by adapting Bruneau et al.'s (2003) Resilience Triangle framework.

Benchmarking Bruneau et al. (2003), the SW-Infra-RA model measures infrastructure resilience by defining and measuring the area of a collective resilience triangle (Fig. 3). In the collective resilience triangle, the vertical axis of the triangle represents the collective functionality of infrastructure, which varies over time. The collective functionality of infrastructure ranges from 0% to 100%, where 100% means no degradation in functions or services and 0% means no service is available. A disaster occurring at time t_0 could cause damage to the infrastructure that the functionality of the infrastructure immediately reduced. The extent to which the functionality is reduced can be measured by the CFL function [Eq. (5)]. The recovery of the infrastructure is a process that takes time, and the infrastructure is completely restored to the original functional level

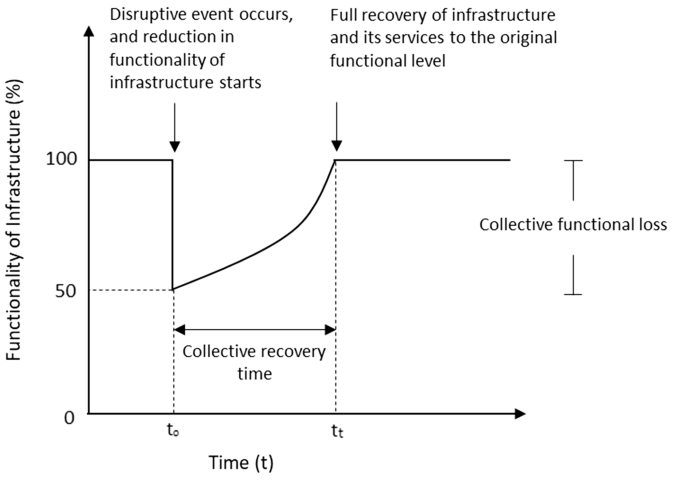

Fig. 3. A conceptual diagram for a collective resilience triangle. (Adapted from Bruneau et al. 2003.)

when it is time t_t. The collective length of recovery (from time t_0 to t_t) can be measured through the CRT function [Eq. (6)].

To measure the area of the collective resilience triangle, the collective loss of infrastructure resilience can be measured through Eq. (7):

$$CLR_k = \int_{t_0}^{t_t} (CFL_k) dt \tag{7}$$

where CLR_k = the collective loss of resilience of infrastructure that serves a group k of multiple communities; CFL_k = the CFL of infrastructure that serves a group k of multiple communities; t_0 = time at which a disruptive event occurs; and t_t = time at which the infrastructure is fully recovered.

If we assume the infrastructure is recovered at a steady pace, the collective loss of infrastructure resilience (CLR) function can be further simplified, as shown in Eq. (8)

$$CLR_k = \frac{CFL_k \times CRT_k}{2} \tag{8}$$

where CLR_k = the collective loss of resilience of infrastructure that serves a group k of multiple communities; CFL_k = the CFL of infrastructure that serves a group k of multiple communities; and CRT_k = the CRT of infrastructure that serves a group k of multiple communities.

As per Eq. (8), a higher value of collective loss of resilience indicates poorer resilience performance of the infrastructure against disasters. In other words, the infrastructure is more likely to experience severe damage, resulting in longer disruptions to the functions and services of the infrastructure.

Case Studies

Hypothetical Case Study

A hypothetical case study was first conducted to illustrate the use of the SW-Infra-RA model in assessing and comparing collective infrastructure resilience across different communities. Hypothetical case studies have been widely used in research in different domains to evaluate or illustrate the use of new methods, models, or frameworks (Balaei et al. 2018; Mostafa and El-Gohary 2014; Zhang and Sanake 2020). This case study aims to analyze and compare the collective resilience of transportation infrastructure in two cities that are composed of various neighborhoods. In this process, we account for the inequality in and vulnerability to disaster impacts among these neighborhoods.

In the case study, Hurricane X caused major damage to the highway infrastructure of City A and City B, which were designed as two hypothetical cities that were composed of 20 neighborhoods each. The highway infrastructure (e.g., roads, highways, bridges) of both cities connects the neighborhoods and supports the socioeconomic development of the local communities. In the event of a disaster, the highway infrastructure plays a vital role by offering links to emergency services, relief, and evacuation routes. The highway infrastructure, however, was in different conditions in City A and City B before being struck by Hurricane X. According to a report on the quality of highway pavement and bridges of City A, approximately 22% of the pavement in City A's highway infrastructure was in "poor" pavement ride quality, and around 17% of bridges were inspected as "structurally deficient." The majority of the pavement and bridges in poor conditions are located in neighborhoods with lower average household income. Further investigation found that these neighborhoods received less financial support for maintaining, repairing, or rehabilitating their highway infrastructure over the last decade. For City B, the report shows that only 4% of the pavement in the city was in "poor" pavement ride quality, while 56% was in "good" quality, and 40% was in "fair" quality. Similarly, only 6% of bridges were inspected as "structurally deficient." The generally good performance of highway infrastructure in City B is attributed to the higher financial support and expenses on maintenance and repair, which may be partially due to relatively better socioeconomic backgrounds (e.g., higher average income, higher housing prices, higher percentages of educated population) of all the neighborhoods in City B.

In the event of Hurricane X, the highway infrastructure of both City A and City B suffered from severe disaster impacts, such as strong wind forces, storm surges, and flash flooding. The damage on the roads, highways, and bridges ranged from pavement failures or structural damage to completely washed-off road sections, which resulted in road and highway closures lasting days to weeks. In City A, disparities in road and highway damage were observed across the 20 neighborhoods. Some neighborhoods suffered from more severe impacts on their highway infrastructure. The roads and bridges were blocked, damaged, or partially washed away due to fallen trees, flying debris, strong storm surges, and flash floods. The road and highway services were disrupted and took three to four weeks to repair before resuming normal operation. On the other hand, some neighborhoods had relatively mild damage, such as erosion of road pavement and poles and trees fallen down on roads. After removing the debris and repairing the damaged roadway segments, the highway infrastructure resumed its normal function. In City B, the road and highway infrastructure across all neighborhoods experienced a similar level of disaster impact. Table 1 presents the hypothetical data on the disaster impacts on the highway infrastructure in the 20 neighborhoods of each city. The data include (1) the percentage of road closures (functional loss); and (2) the time required to resume road services (recovery time).

Utilizing the dataset from Table 1, we followed five steps to assess the resilience of highway infrastructure in Cities A and B. In Step 1, normalization of the values of functional loss (percentage of road closures) and recovery time (time required to resume road services) was conducted to ensure that their units and scales are comparable (the values range between 0 to 1 after normalization). In Step 2, the Gini coefficients of functional loss and recovery time were determined through the Lorenz curve. The Lorenz curves that represent the distributions of road closures and time required for road reopening across the 20 neighborhoods in Cities A and B are depicted in Figs. 4 and 5, respectively. The results of Gini coefficients are summarized in Table 2. As per Table 2, although the average disaster impacts on the highway infrastructure were found to be similar for both cities, higher inequality in disaster impacts was found in City A. In Step 3, the lines of vulnerability for disaster impacts on highway infrastructure were determined using Eqs. (3) and (4). In Step 4, the collective disaster impacts on highway infrastructure in Cities A and B were calculated using Eqs. (5) and (6). A 0.5 coefficient γ (and λ) was employed for the analysis; it represents a medium extent of penalization on the unequal distributions of disaster impacts on highway infrastructure across the 20 neighborhoods in each city. Similarly, a 0.5 coefficient δ (and μ) was used; it represents a medium extent of accounting for the severe impacts on the vulnerable neighborhoods in collective impact analysis. In Step 5, the collective resilience of highway infrastructure for Cities A and B was calculated using Eq. (8). The results of lines of vulnerability, collective disaster impacts, and collective loss of resilience for Cities A and B are summarized in Table 2.

Downloaded from ascelibrary.org by Florida International University on 12/05/22. Copyright ASCE. For personal use only; all rights reserved.

Table 1. Functional loss and recovery time of highway infrastructure of City A and City B

City	Neighborhood	Percentage of road closures (FL) (%)	Time required to resume road services (RT) (days)
City A	A	78	20
	B	68	19
	C	85	24
	D	82	20
	E	96	24
	F	6	8
	G	20	17
	H	14	9
	I	10	8
	J	21	8
	K	95	24
	L	92	19
	M	97	23
	N	88	18
	O	97	18
	P	94	19
	Q	18	10
	R	28	9
	S	13	13
	T	44	6
City B	a	67	19
	b	65	19
	c	62	18
	d	65	18
	e	72	12
	f	63	16
	g	46	13
	h	42	13
	i	44	17
	j	45	12
	k	51	16
	l	57	18
	m	58	15
	n	54	12
	o	58	11
	p	52	15
	q	56	15
	r	49	10
	s	60	14
	t	61	17

These results indicate that the overall resilience performance of the highway infrastructure of City B is better than that of City A as a lower value in loss of resilience represents better resilience performance. The results imply that, collectively, the highway infrastructure of City B had less damage and was more likely to resume its services within a short period of time. It is worth noticing that although the disaster impact data for the 20 neighborhoods of each city have similar average values, City A receives a higher score on collective loss of resilience by using the SW-Infra-RA model. This is mainly due to the inequality or unequal distributions of disaster impacts across different neighborhoods of City A. As per Table 1, neighborhoods M, O, and P of City A had much higher percentages of road closures and also required almost three weeks to fully resume road services, whereas neighborhoods like F, I, and S of City A had minimum road closures and resumed road services within 8 to 10 days. Furthermore, the low resilience performance of City A could be attributed to the severe impacts on the highway infrastructure of some vulnerable neighborhoods in City A, further augmenting the collective disaster impacts. For example, a high percentage of road pavement and bridges in neighborhoods E, K, and M of City A were in poor conditions even before the strike of Hurricane X. Hurricane X further damaged these roads and bridges that were in vulnerable conditions, resulting in a longer time for resuming road services. Thus, more neighborhoods were accounted as vulnerable neighborhoods, as the disaster impacts on these neighborhoods from Hurricane X were above the line of vulnerability.

Hurricane Michael Case Study

A real case study on Hurricane Michael was conducted to assess the collective resilience of electric power systems in 12 counties in the Florida Panhandle region. Hurricane Michael was a Category 5 hurricane that made landfall in the Florida Panhandle region on October 10, 2018 (NHC 2019). Twelve counties (Fig. 6) in this region issued disaster declarations, including Bay, Calhoun, Franklin, Gadsden, Gulf, Holmes, Jackson, Leon, Liberty, Taylor, Wakulla, and Washington Counties. Hurricane Michael brought devastating winds and strong storm surges to these counties, and it caused massive damage and destruction to the infrastructure of the local communities (NHC 2019). According to a report

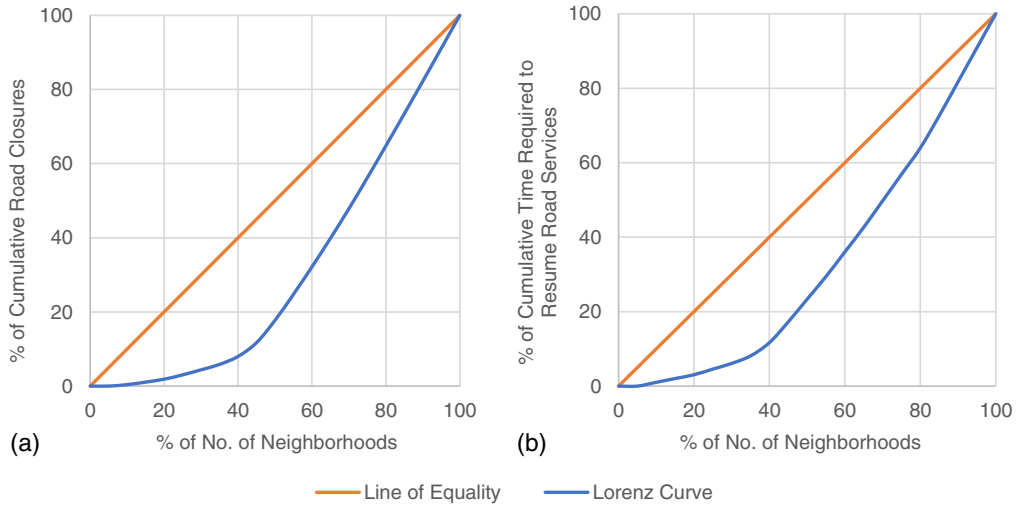

Fig. 4. Lorenz curves for the distribution of disaster impacts in City A due to Hurricane X: (a) A Lorenz curve for the distribution of road closures across neighborhoods in City A due to Hurricane X; and (b) a Lorenz curve for the distribution of time required to resume road services across neighborhoods in City A due to Hurricane X.

Downloaded from ascelibrary.org by Florida International University on 12/05/22. Copyright ASCE. For personal use only; all rights reserved.

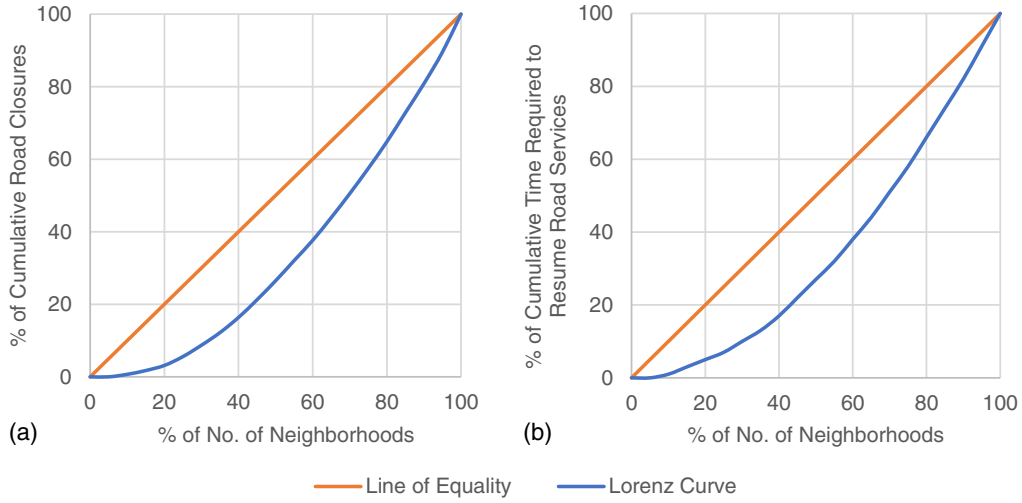

Fig. 5. Lorenz curves for the distribution of disaster impacts in City B due to Hurricane X: (a) A Lorenz curve for the distribution of road closures across neighborhoods in City B due to Hurricane X; and (b) a Lorenz curve for the distribution of time required to resume road services across neighborhoods in City B due to Hurricane X.

Table 2. Results of resilience assessment of highway infrastructure of City A and City B

	City A		City B	
Parameter	Functional loss	Recovery time	Functional loss	Recovery time
Gini coefficient	0.38	0.35	0.32	0.31
Line of vulnerability	0.76	0.72	0.62	0.71
Collective disaster impact	0.71	0.68	0.61	0.67
Collective loss of resilience	0.24		0.19	

(NHC 2019), the inundation height due to the storm surges was estimated to be 9 to 14 feet above ground level in the Florida Panhandle region. It was estimated that Hurricane Michael caused $18.4 billion in damage, primarily incurred due to damage to infrastructure (NWS 2018). The strong wind forces and storm surges caused damage to power substations, resulting in power outages lasting for weeks (FPSC 2021). The physical structures, such as utility poles and transmission towers, were severely damaged and destroyed due to fallen trees, flying debris, and flash floods (Dhakal et al. 2021; Pathak et al. 2020).

In this case study, we selected two disaster impact indicators for analysis: (1) percentage of electric power outages; and (2) time required for resuming electric power services. The data on electric power systems of the 12 Florida counties that issued disaster declarations were collected from Florida Public Service Commission (FPSC 2021). The data are summarized in Table 3. As per Table 3, Hurricane Michael caused disproportionate impacts on the electric power systems of the 12 counties. For example, Calhoun, Gulf, Jackson, and Washington Counties suffered from more severe impacts on their electric power systems, with power outages ranging from 96.19% to 100%. It took more than three weeks for these counties to fully resume their electric power services (FPSC 2021). On the other hand, Taylor County had a relatively lower percentage of power outages (20.14%), and the county was able to resume power transmission and supply rapidly after the hurricane (FPSC 2021).

By using the data in Table 3 and following the five steps as described in the Hypothetical Case Study Section, we performed the resilience assessment of the electric power system of the 12 disaster-impacted counties in three contexts. In Context I, we did not account for inequality in or vulnerability to disaster impacts in the infrastructure resilience assessment. Thus, the coefficients of γ, δ, λ, and μ were assigned to 0, and the coefficients of α and β were assigned to 1. In Context II, we accounted for disaster inequality and vulnerability to a medium extent. Thus, all the coefficients, including α, β, γ, δ, λ, and μ, were assigned to 0.5. In Context III, we fully accounted for disaster inequality and vulnerability in our analysis. Thus, the coefficients of γ, δ, λ, and μ were assigned to 1, and the coefficients of α and β were assigned to 0. Fig. 7 shows the Lorenz curves for the distributions of power outages and the time required to resume electric power services. Table 4 summarizes the results of the resilience assessment in the three defined contexts.

As per Table 4, the results of collective loss of resilience are 0.25, 0.45, and 0.81 in Contexts I, II, and III, respectively. These results show that the performance of the model is sensitive to the intensity of accounting for disaster inequality and vulnerability. The model is designed in a way that allows users to flexibly choose the coefficients that control the intensity of accounting for disaster inequality and vulnerability. For example, if an engineer focuses solely on analyzing the functional loss and recovery time of infrastructure systems without emphasis on inequality and vulnerability among the impacted communities, he/she may assign the coefficients of γ, λ, δ, and μ to 0. Thus, as per Eqs. (5)–(8), the collective loss of resilience of these counties under study would be only based on the average disaster impacts on the infrastructure of those counties. On the other hand, if a planner or a mitigation expert would like to consider disaster inequality and vulnerability, which may inform future recovery and mitigation efforts, he/she may choose to assign a relatively high value (e.g., 1) for the coefficients

Downloaded from ascelibrary.org by Florida International University on 12/05/22. Copyright ASCE. For personal use only; all rights reserved.

Downloaded from ascelibrary.org by Florida International University on 12/05/22. Copyright ASCE. For personal use only; all rights reserved.

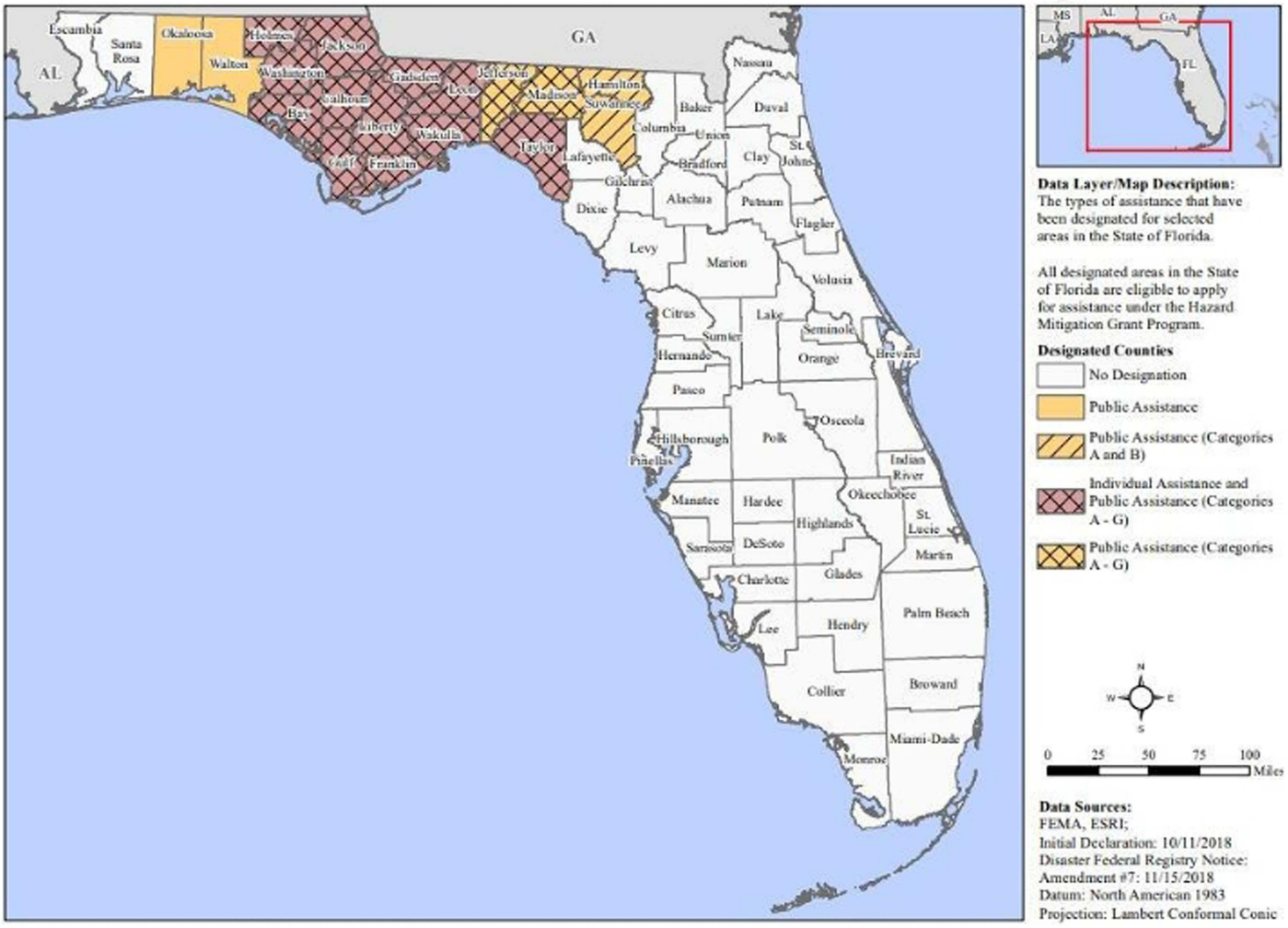

Fig. 6. Counties of the Florida Panhandle region that issued disaster declarations. (Reprinted from FEMA 2018; data sources: FEMA, ESRI.)

Table 3. Functional loss and recovery time of electric power infrastructure in Hurricane Michael

County	Percentage of electric power outages (FL) (%)	Time required to resume electric power services (RT) (days)
Bay	96.6	23
Calhoun	100	27
Franklin	96.79	7
Gadsden	92.12	17
Gulf	99.05	23
Holmes	93.82	12
Jackson	99.78	27
Leon	65.69	14
Liberty	65.94	17
Taylor	20.14	2
Wakulla	93.49	14
Washington	96.19	24

of γ, λ, δ, and μ, thus placing a higher emphasis on the impacts of disaster disparities and vulnerabilities on the collective loss of resilience. In this case, the collective loss of resilience would be augmented as the disproportionate disaster impacts across the counties and the potentially severe disaster impacts on the vulnerable counties are considered negative factors that could exacerbate the collective loss of resilience. It is thus recommended to use a consistent set of coefficients when assessing the resilience of a set of infrastructure alternatives.

In addition, the results show that in the case of Hurricane Michael, the impacts of disaster inequality and vulnerability on the collective loss of resilience of electric power infrastructure were relatively high. The unequal distributions of disaster impacts on electric power infrastructure (including both power outages and time required to resume electric power services) across different counties in Hurricane Michael can be observed through the relatively high Gini coefficients ($G_{FL} = 0.64$ and $G_{RT} = 0.63$). Such disparities in disaster impacts could primarily be caused by the counties' different levels of disaster exposure. In this case study, Hurricane Michael impacted a large geographic region. Counties that are located in close proximity to the hurricane path experienced much significant wind and storm forces compared to counties that are relatively farther away. For example, counties including Calhoun, Gadsden, Gulf, Jackson, and Washington Counties experienced strong storm surges and had an average windspeed of approximately 74 mph (Senkbeil et al. 2020). The percentage of power losses in these counties ranges from 92.12% to 100%. On the other hand, counties, such as Taylor and Leon counties, had relatively lower average wind speeds of approximately 39 mph and 57 mph, respectively (Senkbeil et al. 2020), and their power

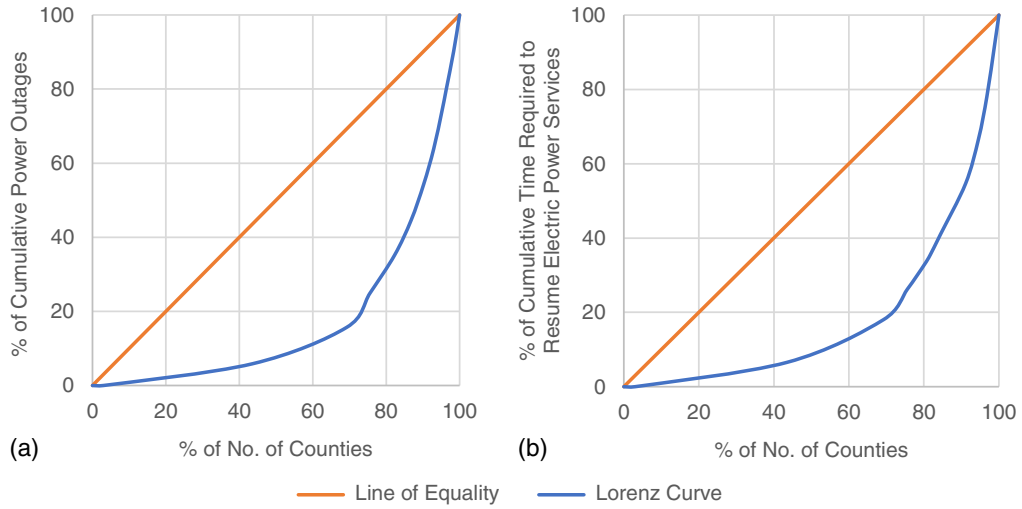

Fig. 7. Lorenz curves for the distribution of disaster impacts due to Hurricane Michael: (a) A Lorenz curve for the distribution of power outages of Florida Panhandle counties due to Hurricane Michael; and (b) a Lorenz curve for the distribution of time required to resume electric power services of Florida Panhandle counties due to Hurricane Michael.

Table 4. Results of resilience assessment of electric power infrastructure in Hurricane Michael

	Context I		Context II		Context III	
Parameter	Functional loss	Recovery time	Functional loss	Recovery time	Functional loss	Recovery time
Gini coefficient	0.64	0.63	0.64	0.63	0.64	0.63
Line of vulnerability	1.00	0.93	0.96	0.77	0.81	0.61
Collective disaster impact	0.81	0.61	1.08	0.83	1.44	1.12
Collective loss of resilience	0.25		0.45		0.81	

losses are 20.14% and 65.69%, respectively. Thus, in a large-scale disaster such as Hurricane Michael, the different levels of disaster exposure are one of the primary reasons that contribute to the disparities in disaster impacts.

Another hidden reason may be the social inequality of these counties. The social inequality situation in Florida is among the worst in the United States and has been getting worse over time (Johnson 2019). In our case, some of the counties (e.g., Gadsden, Calhoun, Franklin, Holmes, and Jackson counties) whose electric power infrastructure suffered from the most severe impacts are also among the most socially vulnerable counties in the region (CDC/ASTDR 2022). In addition, previous research by the authors (Dhakal et al. 2021) has found that the counties with different socioeconomic and demographic characteristics (e.g., age, race, income, health) experienced different levels of infrastructure damage and speeds of recovery. Those counties with higher percentages of socially vulnerable populations experienced a relatively higher level of damage and required a longer time for recovery (Dhakal et al. 2021). Research on other disasters (e.g., Ward and Shivley 2016; Yoon 2012; Flanagan et al. 2011) also show that disaster vulnerability is interrelated with social vulnerability; many social factors (e.g., age, gender, income, and education) may impact the resilience of communities. Under the same level of exposure, communities that are socially vulnerable are more likely to suffer from severe impacts (e.g., higher power outages, traffic disruptions, and higher congestion) (Hallegatte et al. 2019). This may be attributed to the fact that socially vulnerable populations often have the fewest resources for disaster preparedness, live in disaster-prone areas, and lack the social, political, and economic capital needed to withstand, adapt to, and recover from a disaster (SAMSHA 2017).

Research Limitations

We acknowledge four main limitations of the research work, which suggests the necessity of future research. First, the proposed SW-Infra-RA model focuses on assessing infrastructure resilience by accounting for disparities of disaster impacts on infrastructure serving multiple communities and potentially more severe impacts on the infrastructure of vulnerable communities. Although the case study discusses some potential reasons behind disaster inequality and vulnerability, the model currently does not focus on establishing the links/interrelationships between such disparities or vulnerabilities and the social or physical factors behind them. More rigorous and extensive research is needed to further explore the factors behind disaster inequality and vulnerability. Second, the proposed SW-Infra-RA model focuses on assessing collective infrastructure resilience through aggregating disaster impacts on the infrastructure of each individual community it serves. It currently does not account for the interdependencies of infrastructure serving these communities. Other methods, such as the system of system approach or the system network analysis, can be used to measure such interdependencies and can be further integrated into the proposed modeling framework. Third, the SW-Infra-RA model is designed to assess the collective infrastructure resilience of a single type of infrastructure. Assessing the resilience of multiple types of infrastructure may be conducted, depending on the input of the data. For example, if the collected data on disaster impacts are for multiple types of infrastructure, it may be possible to derive the collective resilience of multiple infrastructures. Fourth, the SW-Infra-RA model was currently implemented in analyzing the resilience of highway infrastructure and electric power systems through

Downloaded from ascelibrary.org by Florida International University on 12/05/22. Copyright ASCE. For personal use only; all rights reserved.

two case studies—one hypothetical case study and one real case study—with a limited number of communities. There is a need to further apply the model in analyzing the resilience of different types of infrastructure with a larger number of communities involved. Such application would offer more insight and understanding of how inequality in and vulnerability to disaster impacts could impact infrastructure resilience.

Conclusions and Contributions

This study presents a new social welfare–based infrastructure resilience assessment (SW-Infra-RA) model for assessing the collective resilience of infrastructure serving multiple communities while accounting for inequality in and vulnerability to disaster impacts. The SW-Infra-RA model is theoretically grounded on the social welfare theory and SWFs. The Gini coefficient was adapted to model unequal distributions of disaster impacts on the infrastructure of different communities. The line of vulnerability was proposed and measured by leveraging Cutter et al.'s (2003) work on SoVI to model disaster vulnerability. The collective disaster impact function was then defined by aggregating the impacts on the infrastructure of individual communities while integrating unequal distributions of disaster impacts and potentially more severe impacts on vulnerable communities. The collective disaster impacts were then considered as input into the collective resilience assessment function, which was developed by adapting Bruneau et al.'s (2003) resilience triangle framework. The application of the SW-Infra-RA model was first illustrated through a hypothetical case study that compares the collective resilience of highway infrastructure of two cities impacted by the same disaster. A real case study was further conducted to illustrate the use of the model for assessing the collective resilience of electric power systems in the context of Hurricane Michael.

Although equity in disasters has been extensively discussed in existing disaster literature (e.g., Tate et al. 2021; Gooden et al. 2009; Bullard 2007), there are currently limited studies that mathematically integrate disaster inequality and vulnerability with infrastructure resilience assessment. This research addresses this gap by proposing a new infrastructure resilience assessment framework that measures the collective resilience of infrastructure serving multiple communities while accounting for disaster inequality and vulnerability. It adapted methods from the social science and economics domain to mathematically measure the unequal distributions of disaster impacts across various communities and proposed new ways of evaluating the severe impacts on vulnerable communities (through the line of vulnerability). The mathematical modeling of the concepts of disaster inequality and vulnerability is the key to creating the quantitative links between infrastructure resilience and equity, enabling equitable resilience assessment of infrastructure.

From practical perspectives, the SW-Infra-RA model provides a theoretical basis for equity-incorporated decision making by allowing decision makers to quantitatively assess infrastructure resilience while accounting for inequality and vulnerability. The results generated using this model can be utilized by decision makers to better understand the inequalities during extreme events and to identify the communities that are more vulnerable in such events. The results may also help practitioners recognize how inequality and vulnerability may hinder or impact overall resilience. For example, by applying the model to previous/ongoing disasters, numerical information about disaster inequality and vulnerability of the impacted regions can be derived, thus helping decision makers prioritize disaster assistance, resources for recovery, or future infrastructure and resilience investments to certain communities. By applying the model using simulated data on certain disasters, the results can help decision makers better understand or predict the potential consequences of a possible disaster in certain areas, especially how inequality and vulnerability play their roles in the disaster. Overall, the model may promote equitable resilience planning or hazard mitigation by allowing both the decision makers and the community residents to better understand the links between resilience planning and equity in their communities.

Data Availability Statement

Some data that support the findings of this study are available from the corresponding author upon reasonable request. These data include the data used for the case studies.

Acknowledgments

This material is partially based upon work supported by the National Science Foundation under Grant No. 1933345. Any opinions, findings, and conclusions or recommendations expressed in this material are those of the author(s) and do not necessarily reflect the views of the National Science Foundation.

References

Adler, M. D. 2017. "A better calculus for regulators: From cost-benefit analysis to the social welfare function." In *Duke law school public law & legal theory series*. Amsterdam, Netherlands: Elsevier. https://doi.org/10.2139/ssrn.2923829.

Afonso, H., M. LaFleur, and D. Alarcón. 2015. "Inequality measurement." Accessed October 10, 2021. https://www.un.org/en/development/desa/policy/wess/wess_dev_issues/dsp_policy_02.pdf.

AJMC (American Journal of Managed Care). 2006. "Vulnerable populations: Who are they?" Accessed July 14, 2022. https://www.ajmc.com/view/nov06-2390ps348-s352.

Argyroudis, S. A., D. V. Achillopoulou, V. Livina, and S. A. Mitoulis. 2021a. "Data-driven resilience assessment for transport infrastructure exposed to multiple hazards." In *Bridge maintenance, safety, management, life-cycle sustainability and innovations*, 3267–3274. Boca Raton, FL: CRC Press.

Argyroudis, S. A., G. Nasiopoulos, N. Mantadakis, and S. A. Mitoulis. 2021b. "Cost-based resilience assessment of bridges subjected to earthquakes." *Int. J. Disaster Resilience Built Environ.* 12 (2): 209–222. https://doi.org/10.1108/IJDRBE-02-2020-0014.

Arrow, K. J. 1963. Vol. 12 of *Social choice and individual values*. New Haven, CT: Yale University Press.

ARUP. 2021. "REDi rating system." Accessed June 20, 2021. https://www.arup.com/perspectives/publications/research/section/redi-rating-system.

Assad, A., O. Moselhi, and T. Zayed. 2019. "A new metric for assessing resilience of water distribution networks." *Water* 11 (8): 1701. https://doi.org/10.3390/w11081701.

Atkinson, A., and A. Brandolini. 2010. "On analyzing the world distribution of income." *World Bank Econ. Rev.* 24 (1): 1–37. https://doi.org/10.1093/wber/lhp020.

Balaei, B., S. Wilkinson, R. Potangaroa, N. Hassani, and M. Alavi-Shoshtari. 2018. "Developing a framework for measuring water supply resilience." *Nat. Hazard. Rev.* 19 (4): 04018013. https://doi.org/10.1061/(ASCE)NH.1527-6996.0000292.

Berkeley, A. R., M. Wallace, and C. Coo. 2010. "A framework for establishing critical infrastructure resilience goals." In *Final report and recommendations by the council, national infrastructure advisory council*, 18–21. Arlington, VA: National Infrastructure Advisory Council.

Braese, J. M., J. E. Maruyama Rentschler, and S. Hallegatte. 2019. "Resilient infrastructure for thriving firms: A review of the evidence."

Downloaded from ascelibrary.org by Florida International University on 12/05/22. Copyright ASCE. For personal use only; all rights reserved.

In *Global facility for disaster reduction and recovery: Policy research working paper*, 8895. Washington, DC: World Bank.

Bruneau, M., S. E. Chang, R. T. Eguchi, G. C. Lee, T. D. O'Rourke, A. M. Reinhorn, M. Shinozuka, K. Tierney, W. A. Wallace, and D. Von Winterfeldt. 2003. "A framework to quantitatively assess and enhance the seismic resilience of communities." *Earthquake Spectra* 19 (4): 733–752. https://doi.org/10.1193/1.1623497.

Bullard, R. D. 2007. "Equity, unnatural man-made disasters, and race: Why environmental justice matters." In *Equity and the environment*. Bradford, UK: Emerald Group Publishing.

Callan, T., and B. Nolan. 1991. "Concepts of poverty and the poverty line." *J. Econ. Surv.* 5 (3): 243–261. https://doi.org/10.1111/j.1467-6419.1991.tb00134.x.

Cardoni, A., G. P. Cimellaro, M. Domaneschi, S. Sordo, and A. Mazza. 2020. "Modeling the interdependency between buildings and the electrical distribution system for seismic resilience assessment." *Int. J. Disaster Risk Reduct.* 42 (Jan): 101315. https://doi.org/10.1016/j.ijdrr.2019.101315.

CCSF (City and County of San Francisco). 2021. "Hazus: A tool for modeling damages and economic losses from natural disasters." Accessed October 05, 2021. https://sfcontroller.org/sites/default/files/FileCenter/Documents/6356-HAZUS%20Presentation.pdf.

CDC/ATSDR (Centre for Disease Control/Agency for Toxic Substances and Disease Registry). 2022. "CDC/ATSDR social vulnerability index." Accessed May 20, 2022. https://www.atsdr.cdc.gov/placeandhealth/svi/index.html.

Chandramouleeswaran, K. R., and H. T. Tran. 2018. "Data-driven resilience quantification of the US Air transportation network." In *Proc., Annual IEEE Int. Systems Conf.*, 1–7. New York: IEEE.

Cimellaro, G. P., A. M. Reinhorn, and M. Bruneau. 2010. "Seismic resilience of a hospital system." *Struct. Infrastruct. Eng.* 6 (1–2): 127–144. https://doi.org/10.1080/15732470802663847.

Coleman, N., A. Esmalian, and A. Mostafavi. 2020. "Equitable resilience in infrastructure systems: Empirical assessment of disparities in hardship experiences of vulnerable populations during service disruptions." *Nat. Hazard. Rev.* 21 (4): 04020034. https://doi.org/10.1061/(ASCE)NH.1527-6996.0000401.

Conceição, P., and P. Ferreira. 2000. *The young person's guide to the Theil index: Suggesting intuitive interpretations and exploring analytical applications*. UTIP Working Paper No. 14. Amsterdam, Netherlands: Elsevier. https://doi.org/10.2139/ssrn.228703.

Cutter, S. L., B. J. Boruff, and W. L. Shirley. 2003. "Social vulnerability to environmental hazards." *Social Sci. Q.* 84 (2): 242–261. https://doi.org/10.1111/1540-6237.8402002.

Deardorff, A. V. 2016. "Deardorffs' glossary of international economics." Accessed September 20, 2021. http://www-personal.umich.edu/~alandear/glossary/w.html.

Decò, A., P. Bocchini, and D. M. Frangopol. 2013. "A probabilistic approach for the prediction of seismic resilience of bridges." *Earthquake Eng. Struct. Dyn.* 42 (10): 1469–1487. https://doi.org/10.1002/eqe.2282.

Dhakal, S., L. Zhang, and X. Lv. 2021. "Understanding infrastructure resilience, social equity, and their interrelationships: Exploratory study using social media data in Hurricane Michael." *Nat. Hazard. Rev.* 22 (4): 04021045. https://doi.org/10.1061/(ASCE)NH.1527-6996.0000512.

Dolan, P., and A. Robinson. 2001. "The measurement of preferences over the distribution of benefits: The importance of the reference point." *Eur. Econ. Rev.* 45 (9): 1697–1709. https://doi.org/10.1016/S0014-2921(00)00052-0.

FEMA. 2018. "Designated areas: Disaster 4399." Accessed June 10, 2021. https://www.fema.gov/disaster/4399/designated-areas.

FEMA. 2021. "FEMA preliminary damage assessment guide." Accessed September 10, 2021. https://www.fema.gov/sites/default/files/documents/fema_2021-pda-guide.pdf.

Fisher, R., and M. Norman. 2010. "Developing measurement indices to enhance protection and resilience of critical infrastructure and key resources." *J. Bus. Continuity Emergency Plann.* 4 (3): 191–206.

Flanagan, B. E., E. W. Gregory, E. J. Hallisey, J. L. Heitgerd, and B. Lewis. 2011. "A social vulnerability index for disaster management." *J. Homeland Secur. Emergency Manage.* 8 (1): 3–15. https://doi.org/10.2202/1547-7355.1792.

FPSC (Florida Public Service Commission). 2021. "Hurricane season power outage reports." Accessed February 10, 2021. http://www.psc.state.fl.us/Home/HurricaneReport.

Füssel, H. M. 2006. "Social welfare functions in global climate-economy models: Methodological inconsistencies and their policy implications." Accessed September 2, 2021. https://ssrn.com/abstract=900023.

GBCI (Green Building Certification Inc.). 2021. "Resilient design for a changing world." Accessed June 14, 2021. https://gbci.org/reli.

Gooden, S., D. Jones, K. J. Martin, and M. Boyd. 2009. "Social equity in local emergency management planning." *State Local Gov. Rev.* 41 (1): 1–12. https://doi.org/10.1177/0160323X0904100101.

Hallegatte, S., J. Rentschler, and J. Rozenberg. 2019. "Lifelines: The resilient infrastructure opportunity." In *Sustainable infrastructure*. Washington, DC: World Bank.

Hao, H., S. Baireddy, E. R. Bartusiak, L. Konz, K. LaTourette, M. Gribbons, M. Chan, M. L. Comer, and E. J. Delp. 2020. "An attention-based system for damage assessment using satellite imagery." Preprint, submitted April 14, 2020. https://arxiv.org/abs/2004.06643.

Harsanyi, J. C. 1955. "Cardinal welfare, individualistic ethics, and interpersonal comparisons of utility." *J. Political Econ.* 63 (4): 309–321. https://doi.org/10.1086/257678.

Hirsch, J. A., G. F. Green, M. Peterson, D. A. Rodriguez, and P. Gordon-Larsen. 2017. "Neighborhood sociodemographics and change in built infrastructure." *J. Urbanism: Int. Res. Placemaking Urban Sustainability* 10 (2): 181–197.

Holling, C. S. 1973. "Resilience and stability of ecological systems." In *Annual review of ecology and systematics*, 1–23. San Mateo, CA: Annual Reviews.

Holling, C. S. 1996. "Engineering resilience versus ecological resilience." In Vol. 31 of *Engineering within ecological constraints*, 32. Washington DC: National Academy of Science.

Hoover, E. M. 1941. "Interstate redistribution of population: 1850-1940." *J. Econ. History* 1 (2): 199–205. https://doi.org/10.1017/S0022050700052980.

Hossain, N. U. I., R. Jaradat, S. Hosseini, M. Marufuzzaman, and R. K. Buchanan. 2019. "A framework for modeling and assessing system resilience using a Bayesian network: A case study of an interdependent electrical infrastructure system." *Int. J. Crit. Infrastruct. Prot.* 25 (Jun): 62–83. https://doi.org/10.1016/j.ijcip.2019.02.002.

Hosseini, S., and K. Barker. 2016. "Modeling infrastructure resilience using Bayesian networks: A case study of inland waterway ports." *Comput. Ind. Eng.* 93 (Jan): 252–266. https://doi.org/10.1016/j.cie.2016.01.007.

Huang, C., and R. Taylor. 2019. "Any federal infrastructure package should boost investment in low-income communities." Accessed June 10, 2021. https://www.cbpp.org/research/federal-budget/any-federal-infrastructure-package-should-boost-investment-in-low-income.

Jacobson, A., A. D. Milman, and D. M. Kammen. 2005. "Letting the (energy) Gini out of the bottle: Lorenz curves of cumulative electricity consumption and Gini coefficients as metrics of energy distribution and equity." *Energy Policy* 33 (14): 1825–1832. https://doi.org/10.1016/j.enpol.2004.02.017.

Jagtenberg, C. J. 2017. "Efficiency and fairness in ambulance planning." Doctoral dissertation, Dutch National Research Institute for Mathematics and Computer Science, VU Amsterdam.

Jian, J. I. N., W. A. N. G. Jianxiang, M. A. Xiaoyi, W. A. N. G. Yuding, and L. I. Renyong. 2015. "Equality of medical health resource allocation in China based on the Gini coefficient method." *Iran. J. Public Health* 44 (4): 445.

Johnson, A. E. 2019. "Florida's rising tide: Income inequality effects by county." *Honors Undergraduate Theses*. Accessed November 10, 2021. https://stars.library.ucf.edu/honorstheses/521.

Kangior, M. 2013. "Engineering resilience: The resilience STARTM home pilot project." Accessed July 25, 2020. https://www.dhs.gov/blog/2013/11/18/engineering-resilience-resilience-star%E2%84%A2-home-pilot-project.

Karamouz, M., M. Taheri, P. Khalili, and X. Chen. 2019. "Building infrastructure resilience in coastal flood risk management." *J. Water Resour.*

Downloaded from ascelibrary.org by Florida International University on 12/05/22. Copyright ASCE. For personal use only; all rights reserved.

Plann. Manage. 145 (4): 04019004. https://doi.org/10.1061/(ASCE)WR.1943-5452.0001043.

Kinjo, K., and T. Ebina. 2017. "Optimal program for autonomous driving under Bentham- and Nash-type social welfare functions." *Procedia Comput. Sci.* 112 (Mar): 61–70. https://doi.org/10.1016/j.procs.2017.08.024.

Kwasinski, A. 2011. "Field damage assessments as a design tool for information and communications technology systems that are resilient to natural disasters." In *Proc., 4th Int. Symp. on Applied Sciences in Biomedical and Communication Technologies*, 1–6. New York: Association for Computing Machinery.

Lam, C. Y., and K. Tai. 2018. "Modeling infrastructure interdependencies by integrating network and fuzzy set theory." *Int. J. Crit. Infrastruct. Prot.* 22 (Mar): 51–61. https://doi.org/10.1016/j.ijcip.2018.05.005.

Maass, W., J. Parsons, S. Purao, V. C. Storey, and C. Woo. 2018. "Data-driven meets theory-driven research in the era of big data: Opportunities and challenges for information systems research." *J. Assoc. Inf. Syst.* 19 (12): 1. https://doi.org/10.17705/1jais.00526.

MacKenzie, C. A., and K. Barker. 2013. "Empirical data and regression analysis for estimation of infrastructure resilience with application to electric power outages." *J. Infrastruct. Syst.* 19 (1): 25–35. https://doi.org/10.1061/(ASCE)IS.1943-555X.0000103.

Mao, Q., and N. Li. 2018. "Assessment of the impact of interdependencies on the resilience of networked critical infrastructure systems." *Nat. Hazards* 93 (1): 315–337. https://doi.org/10.1007/s11069-018-3302-3.

Massarra, C. C. 2012. "Hurricane damage assessment process for residential buildings." Master's thesis, Agriculture and Mechanical College, Louisiana State Univ. https://digitalcommons.lsu.edu/gradschool_theses/520.

Mawgoud, A. A., M. M. Eltabey, and A. Abu-Talleb. 2021. "A distributed artificial intelligence framework to evolve infrastructure resilience in telecommunications sector." In *Proc., Int. Conf. on Advanced Machine Learning Technologies and Applications*, 774–784. New York: Springer.

Meerow, S., and J. P. Neweell. 2019. "Urban resilience for whom, what, when, where, and why?" *Urban Geogr.* 40 (3): 309–329. https://doi.org/10.1080/02723638.2016.1206395.

Meerow, S., P. Pajouhesh, and T. R. Miller. 2019. "Social equity in urban resilience planning." *Local Environ.* 24 (9): 793–808. https://doi.org/10.1080/13549839.2019.1645103.

Mostafa, M. A., and N. M. El-Gohary. 2014. "Stakeholder-sensitive social welfare–oriented benefit analysis for sustainable infrastructure project development." *J. Constr. Eng. Manage.* 140 (9): 04014038. https://doi.org/10.1061/(ASCE)CO.1943-7862.0000788.

Mottahedi, A., F. Sereshki, M. Ataei, A. Nouri Qarahasanlou, and A. Barabadi. 2021. "The Resilience of critical infrastructure systems: A systematic literature review." *Energies* 14 (6): 1571. https://doi.org/10.3390/en14061571.

Nexus. 2017. "Hurricane Harvey hit low-income communities hardest." Accessed October 10, 2021. https://archive.thinkprogress.org/hurricane-harvey-hit-low-income-communities-hardest-6d13506b7e60/.

NHC (National Hurricane Center). 2019. "Hurricane Michael." Accessed July 5, 2021. https://www.nhc.noaa.gov/data/tcr/AL142018_Michael.pdf.

Nicholson, G. 2014. "Inequality and its impact on the resilience of societies." Accessed November 4, 2021. https://eturbonews.com/inequality-and-its-impact-resilience-societies/.

Nogal, M., A. O'Connor, B. Martinez-Pastor, and B. Caulfield. 2017. "Novel probabilistic resilience assessment framework of transportation networks against extreme weather events." *ASCE-ASME J. Risk Uncertainty Eng. Syst. Part A: Civ. Eng.* 3 (3): 04017004. https://doi.org/10.1061/AJRUA6.0000908.

NWS (National Weather Service). 2018. "Catastrophic Hurricane Michael Strikes Florida Panhandle October 10, 2018." Accessed June 10, 2021. https://www.weather.gov/tae/HurricaneMichael2018.

Ouyang, M., and L. Duenas-Osorio. 2014. "Multi-dimensional hurricane resilience assessment of electric power systems." *Struct. Saf.* 48 (Jun): 15–24. https://doi.org/10.1016/j.strusafe.2014.01.001.

Panteli, M., P. Mancarella, D. N. Trakas, E. Kyriakides, and N. D. Hatziargyriou. 2017. "Metrics and quantification of operational and infrastructure resilience in power systems." *IEEE Trans. Power Syst.* 32 (6): 4732–4742. https://doi.org/10.1109/TPWRS.2017.2664141.

Pathak, A., L. Zhang, and N. E. Ganapati. 2020. "Understanding multi-sector stakeholder value dynamics in Hurricane Michael to facilitate collaborative decision making in disaster contexts." *Nat. Hazard. Rev.* 21 (3): 04020032. https://doi.org/10.1061/(ASCE)NH.1527-6996.0000400.

Petit, F. D., L. K. Eaton, R. E. Fisher, S. F. McAraw, and M. J. Collins III. 2012. "Developing an index to assess the resilience of critical infrastructure." *Int. J. Risk Assess. Manage.* 16 (1–3): 28–47. https://doi.org/10.1504/IJRAM.2012.047551.

Planitz, A. 1999. "A guide to successful damage and needs assessment." Accessed January 20, 2022. https://haitilearning.alnap.org/system/files/content/resource/files/main/1997_spdrp_a_guide_for_succesfull_damage_and_needs_assessment.pdf.

Rao, K. D., S. Makimoto, M. Peters, G. M. Leung, G. Bloom, and Y. Katsuma. 2019. "Vulnerable populations and universal health coverage." In *Leave no one behind: Time for specifics on the sustainable development goals*. Washington, DC: Brookings Institution Press.

Rawls, J. 1971. *A theory of justice*. Cambridge, MA: Harvard University Press.

Rehak, D., P. Senovsky, M. Hromada, and T. Lovecek. 2019. "Complex approach to assessing resilience of critical infrastructure elements." *Int. J. Crit. Infrastruct. Prot.* 25 (Jun): 125–138. https://doi.org/10.1016/j.ijcip.2019.03.003.

RF (The Rockefeller Foundation). 2021. "100 resilient cities." Accessed June 2, 2021. https://www.rockefellerfoundation.org/our-work/initiatives/100-resilient-cities/.

SAMSHA (Substance Abuse and Mental Health Services Association). 2017. "Greater impact: How disasters affect people of low socioeconomic status." Accessed July 10, 2021. https://www.samhsa.gov/sites/default/files/dtac/srb-low-ses_2.pdf.

Schneider, M., and B.-C. Kim. 2020. "The utilitarian–maximin social welfare function and anomalies in social choice." *South. Econ. J.* 87 (2): 629–646. https://doi.org/10.1002/soej.12464.

Sen, A. 1997. *On economic inequality*. Oxford, UK: Oxford University Press.

Senkbeil, J. C., L. Myers, S. Jasko, J. R. Reed, and R. Mueller. 2020. "Communication and hazard perception lessons from category five hurricane Michael." *Atmosphere* 11 (8): 804. https://doi.org/10.3390/atmos11080804.

Shang, Q., T. Wang, and J. Li. 2020. "A quantitative framework to evaluate the seismic resilience of hospital systems." *J. Earthquake Eng.* 26 (7): 3364–3388. https://doi.org/10.1080/13632469.2020.1802371.

Shin, S., S. Lee, D. R. Judi, M. Parvania, E. Goharian, T. McPherson, and S. J. Burian. 2018. "A systematic review of quantitative resilience measures for water infrastructure systems." *Water* 10 (2): 164. https://doi.org/10.3390/w10020164.

Tate, E., M. A. Rahman, C. T. Emrich, and C. C. Sampson. 2021. "Flood exposure and social vulnerability in the United States." *Nat. Hazards* 106 (1): 435–457. https://doi.org/10.1007/s11069-020-04470-2.

Theil, H. 1967. *Economics and information theory*. No. 04, HB74. M3, T4. Amsterdam, Holland: North Holland Publishing Company.

Tonn, G., J. Czajkowski, H. Kunreuther, K. Angotti, and K. Gelman. 2020. "Measuring transportation infrastructure resilience: Case study with Amtrak." *J. Infrastruct. Syst.* 26 (1): 05020001. https://doi.org/10.1061/(ASCE)IS.1943-555X.0000526.

Trapeznikova, I. 2019. *Measuring income inequality*. Bonn, Germany: IZA, World of Labor. https://doi.org/10.15185/izawol.462.

Tselios, V., and E. L. Tompkins. 2019. "What causes nations to recover from disasters? An inquiry into the role of wealth, income inequality, and social welfare provisioning." *Int. J. Disaster Risk Reduct.* 33 (Feb): 162–180. https://doi.org/10.1016/j.ijdrr.2018.10.003.

UNCTAD (United Nations Conference on Trade and Development). 2021. "The many faces of inequality." Accessed May 15, 2022. https://sdgpulse.unctad.org/in-focus-inequality/#Ref_Cobham2013.

USRC (US Resiliency Council). 2021. "Resilient communities need resilient buildings." Accessed July 25, 2021. http://www.usrc.org/.

Wang, X.-J., J.-Y. Zhang, S. Shahid, A. ElMahdi, R.-M. He, X.-G. Wang, and M. Ali. 2012. "Gini coefficient to assess equity in domestic

Downloaded from ascelibrary.org by Florida International University on 12/05/22. Copyright ASCE. For personal use only; all rights reserved.

water supply in the Yellow River." *Mitigation Adapt. Strategies Global Change* 17 (1): 65–75. https://doi.org/10.1007/s11027-011-9309-7.
Ward, P. S., and G. E. Shively. 2016. "Disaster risk, social vulnerability, and economic development." *Disasters* 41 (2): 324–351. https://doi.org/10.1111/disa.12199.
Wescoat, J., et al. 2018. "Equitable Resilience, 2018-2021." Accessed June 6, 2022. https://lcau.mit.edu/equitableresilience.
Weymark, J. A. 2016. "Social welfare functions." *The Oxford handbook of well-being and public policy*, 126–159. Oxford, England: Oxford University Press.
Wodon, Q., and S. Yitzhaki. 2008. "Inequality in multidimensional indicators of well-being: Methodology and application to the human development index." In *Modeling income distributions and Lorenz curves*, 303–317. New York: Springer.
Yang, Y., W. Tang, Y. Liu, Y. Xin, and Q. Wu. 2018. "Quantitative resilience assessment for power transmission systems under typhoon weather." *IEEE Access* 6 (May): 40747–40756. https://doi.org/10.1109/ACCESS.2018.2858860.
Yoon, D. K. 2012. "Assessment of social vulnerability to natural disasters: A comparative study." *Nat. Hazards* 63 (2): 823–843. https://doi.org/10.1007/s11069-012-0189-2.
Zamanian, S., M. Rahimi, and A. Shafieezadeh. 2020. "Resilience of sewer networks to extreme weather hazards: Past experiences and an assessment framework." In *Proc., Pipelines 2020*, 50–59. Reston, VA: ASTM.
Zhang, L., and S. Sanake. 2020. "Social welfare-based human comfort aggregation model to facilitate healthy and comfortable indoor environments." *J. Archit. Eng.* 26 (3): 04020027. https://doi.org/10.1061/(ASCE)AE.1943-5568.0000422.
Zhu, Y., K. Xie, K. Ozbay, F. Zuo, and H. Yang. 2017. "Data-driven spatial modeling for quantifying networkwide resilience in the aftermath of hurricanes Irene and Sandy." *Transp. Res. Rec.* 2604 (1): 9–18. https://doi.org/10.3141/2604-02.

Downloaded from ascelibrary.org by Florida International University on 12/05/22. Copyright ASCE. For personal use only; all rights reserved.